# Computer-Aided Detection Of Pulmonary Tuberculosis and Pulmonary Cavity on Adult Chest Radiographs using a Region Convolutional Neural Network*

Kevin Eric R. Santos, MD[1]


## ABSTRACT

**Objectives:** To train and evaluate the performance of a detector for pulmonary tuberculosis and pulmonary cavity, using the Faster Region Convolutional Neural Network model.

**Methods**

**Study Design:** A cross-sectional study design was employed to describe the sensitivity, specificity, and accuracy of the Faster Region Convolutional Neural Network model for the detection of pulmonary tuberculosis and pulmonary cavity.

**Subjects:** Radiographs for the training dataset and testing dataset were acquired from the Picture Archiving and Communication System of the a general public hospital in Quezon City.

**Setting:** The setting of the study is a general public hospital in Quezon City, Philippines.

**Outcomes:** The detector for pulmonary tuberculosis and pulmonary cavity was trained with the training dataset using the TensorFlow machine learning library, with the Faster-RCNN-Inception-V2 used as the base model.

Detector findings on the testing dataset were compared and analyzed against findings of three board-certified radiologists.

**Results:** The detector achieved 92.11% sensitivity, 87.1% specificity, and 89% accuracy as a screening tool, and 84.04% sensitivity, 98.04% specificity, and 95.87% accuracy, as a locator of pulmonary tuberculosis and cavity.

**Conclusion**: This study is the first of its kind to demonstrate the feasibility of training a detector for pulmonary tuberculosis and pulmonary cavities using the Region Convolutional Neural Network model. Limitations and improvements to the detector may be addressed in future research.


**Keywords:** Tuberculosis, Pulmonary, Sensitivity and Specificity, Neural Networks (Computer), Software

## INTRODUCTION

Pulmonary tuberculosis (PTB) remains one of the illnesses with high disease burden in the Philippines. According to the 2016 National Tuberculosis Prevalence Survey, the prevalence of PTB in the Philippines is 10.6 per 1000 persons, which is an increase from the previously measured prevalence of 4.7 per 1000 persons in 2007 [1]. Radiology plays a vital role in the diagnosis of the disease. The chest radiograph and sputum smear and culture are the initial diagnostic tests for patients suspected of PTB.

Several studies on computer-aided detection of PTB on chest radiographs have been published. CAD4TB by Delft Imaging Systems, is the only commercial software package on the market for computer-aided detection of PTB. A systematic review investigating 5 studies on the software, showed that CAD4TB demonstrates middle to high sensitivity (47-100%), and inconsistent specificity (23-94%). Concerns were raised regarding the generalizability of the software to populations other than those used to train it. The review concludes that evidence to support the use of computer-aided detection in PTB diagnosis is limited and that more research in the field is needed. [2] In recent years, the convolutional neural network (CNN) has been the

*2nd Place, 2020 Philippine Medical Association Original Research Presentation, September 7, 2020

[1]Resident, Quirino Memorial Medical Center, Quezon city

most successful computational algorithm used in computer vision research.[3] Two studies were published applying a CNN to PTB detection. Research by Hwang et al. in 2016 pioneered the use of a CNN in detecting PTB and achieved an area-under-curve (AUC) of 0.964[4]. A similar study by Lakhani et al. in 2017, demonstrated a higher AUC of 0.99, with 97% sensitivity and 100% specificity[5]. The limitation of using CNN is that it can accurately classify PTB, but cannot explicitly point out the location of the disease. The Region Convolutional Neural Network (R-CNN) is an algorithm derived from CNN capable of identifying the location of the object of interest within a larger image. Several iterations on the R-CNN algorithm have been developed, namely the Fast R-CNN and the Faster R-CNN. The latest iteration of this algorithm is the Faster R-CNN, which is as accurate, but is capable of detection at higher speed than earlier versions.[6]

The objectives of this study are: 1) to train a detector for PTB opacities and pulmonary cavity based on the Faster R-CNN model, and 2) to test the sensitivity, specificity, and percent accuracy of the detector as a screening tool and as a locator for PTB opacities and pulmonary cavities.

## SIGNIFICANCE OF THE STUDY

While researches were published exploring the application of CNN in PTB detection, no study yet exists on the application of R-CNN to the problem of PTB detection.

In addition to bridging this gap in knowledge, there are also other compelling reasons to conduct research in the field of computer-aided detection in medical imaging. Novel systems need to be assessed for sensitivity, specificity, and accuracy. Off-the-shelf commercial software for PTB detection are expensive and may not be applicable to the local population, hence the need to create detectors trained with radiographs of the local population.

Development of such software may be integrated into public health screening programs for PTB, and may be utilized in areas where radiologists are unavailable.

## MATERIALS AND METHODS

The methodology of this study proceeds in two phases:

1. Training the Faster R-CNN based classifier for detection of PTB and pulmonary cavities. (see Figure 1)
2. Verification of detector findings, against the findings of a panel of 3 board certified radiologists. (see Figure 2)

### *Training the Faster R-CNN based detector*

#### Systematic search for chest radiographs with PTB and pulmonary cavities

A systematic search through official results of chest radiographs done in a general public hospital in Quezon City, from January 2016 to January 2018 was performed. Search terms used were "PTB", "cavity", "cavitation" and "cavitary". This yielded an initial pool of 816 radiographs.

Inclusion and exclusion criteria were applied, after which only 654 radiographs were included. Only initial chest radiographs of adults 19 years old and above, taken in an upright or sitting position in either anteroposterior or posteroanterior views, were included, while radiographs with medical devices superimposing the lung parenchyma such as electrodes, wires, tubes and catheters, were excluded.

#### Collection, processing and annotation of sample chest radiographs

The 654 chest radiographs included in the study were downloaded from the picture archiving and communications system (PACS) in Digital Imaging and Communications in Medicine (DICOM) format. Age, sex, hospital number, and accession number of the radiographs were encoded. Names of patients were removed, anonymizing the dataset. These were then converted to jpeg files with the program MicroDicom viewer[7].

Histogram equalization and reduction in size to 600 pixels height, with aspect ratio

maintained for image width, were performed with the software GIMP 2.10.8[8].

Out of the 654 images, 100 images were randomly selected and set aside to form part of the testing dataset. Random selection was done with Microsoft Excel, by assigning pseudorandom numbers to each radiograph via the *rand()* function and sorting the radiographs in an ascending manner based on the generated pseudorandom numbers. The first 100 radiographs with the smallest pseudorandom numbers were selected and set aside for testing, while the remaining 554 images would comprise the training dataset.

The images in the training dataset were then annotated with the program LabelImg[9]. Bounding boxes were placed around findings of PTB opacities and pulmonary cavities, based on the text of the official result of each radiograph.

### Training the PTB and cavity detector

The images were loaded onto a computer with the following specifications: Windows 7 64-bit operating system, Intel Core i7-6700 CPU, 1TB of hard disk space, and 8GB of RAM.

Training process and source code used for training were adapted from the process described by Juras[10], which used the object detection module of the open source machine learning library, TensorFlow. The Faster-RCNN-Inception-V2 was used as the base model.

The detector was trained with the 554 training images for 38 epochs.

## *Testing the PTB and cavity detector*

### Overview of testing methodology

The PTB and cavity detector was tested on a randomized set of radiographs composed of approximately one-third radiographs with PTB and/or cavity, one-third radiographs with pathology other than PTB and cavity, and one-third negative chest radiographs. The findings of the detector were then verified by a panel of three board-certified radiologists.

### Sample size calculation

Sample size calculation for the number of testing radiographs was determined using the tables for minimum sample size for sensitivity and specificity analysis, as determined by Bujang[11] (see Appendix 1). Minimum sample size was 67 test radiographs using parameters of 30% prevalence, minimum sensitivity of 80%, and 80% power.

### Preparation and randomization of test images

A systematic search through official results of chest radiographs done in a general public hospital in Quezon City from January 2016 to January 2018 was performed for 1) negative chest radiographs and 2) pathologic chest radiographs without PTB and cavity. This initial search yielded 10,000 results for each category.

One hundred radiographs from each category were randomly selected using the previously described randomization process using Microsoft Excel. These were downloaded from the PACS as DICOM format and processed in the same manner as radiographs in the training dataset.

These were pooled with the 100 radiographs with PTB and pulmonary cavity set aside previously. From this pool of 300 chest radiographs, 100 radiographs were randomly selected, using the same randomization process.

The final set of test images is a heterogeneous set of 100 radiographs composed of 32 radiographs with PTB and/or cavity, 36 negative chest radiographs, and 32 pathologic non-PTB non-cavity chest radiographs. Pathologic non-PTB non-cavity radiographs comprise a myriad of pathologies, such as pneumonia, pleural effusion, bronchitis/bronchiectasis, pulmonary congestion, fibrosis, subsegmental atelectasis, and fibrosis (see Table 1).

### Application of the detector to the test images

The detector was then applied to the test images, using the object detection module within TensorFlow. Coordinates of bounding boxes representing areas with PTB and cavity were

determined by the detector, and were drawn onto the image file using the module OpenCV[12], producing the final output images (see Figure 3).

### Verification of detector findings

Verification of the detector findings was performed by three board-certified radiologists of the Philippine College of Radiology, each with 5-6 years of training and experience in radiology. Each radiologist was given the set of final output images, and a verification sheet with the list of findings per image (see Appendix 2). Each finding was then verified as either true or false. In addition, the verifying radiologist was asked to note any missed PTB opacities or cavity. For each finding, at least 2 out of 3 verifying radiologists must be in agreement to be valid.

Each bounding box was classified into one of the following categories:

- True negative finding - The detector did not identify any finding, confirmed by the verifying radiologists.
- True positive finding - The detector identified a PTB opacity or cavity, confirmed by the verifying radiologists.
- False negative finding - The detector did not identify any finding on the radiograph, but verifying radiologists identified a missed PTB opacity or cavity.
- False positive finding - The detector identified a PTB opacity or cavity, but verifying radiologists disagreed with the finding.

## Data Analysis

The results of verification were analyzed in two different ways, in accordance with the study objectives.

First, the data was analyzed as a screening tool for PTB, utilizing the chest radiograph as the unit of analysis, and making use of lenient parameters for classification. Each chest radiograph in the final set of test images was classified into one of the following categories (see Figure 4):

- True Negative Radiograph - The radiograph contains no findings.
- True Positive Radiograph - The radiograph contains at least one true positive finding. If false positive and false negative findings are also present, the radiograph is still counted as a true positive.
- False Negative Radiograph - The radiograph contains at least one false negative finding.
- False Positive Radiograph - The radiograph contains at least one false positive finding. If there is also a false negative finding, the radiograph is still classified as a false positive.

Second, the data was analyzed as to its performance in locating PTB opacities and cavities on chest radiographs. The lungs on each radiograph were divided into 6 parts based on location and laterality, into upper, middle, and lower lungs on the left or the right. Each one-sixth region formed the unit of analysis for analysis as locator. Bounding boxes are determined to be within the lung region if greater than 50% of the box area is within the lung region.

Each one-sixth portion were classified as follows, based on radiologist verification (see Figure 5 for examples):

- True Negative Lung Region - The lung region contains no findings.
- True Positive Lung Region- The lung region contains at least one true positive finding.
- False Negative Lung Region - The lung region contains a missed PTB opacity or cavity.
- False Positive Lung Region - The lung region contains a finding verified to be a false positive.

If a region is classified into two or more groups, it will be classified by the largest box by

area. If a finding is detected outside the bounds of the lungs, it is counted as an additional false positive.

After classification, 2x2 contingency tables were used to derive sensitivity, specificity, and accuracy.

## RESULTS

As a screening tool, the trained detector for PTB opacities and pulmonary cavity demonstrated 92.11% sensitivity, 87.1% specificity, and 89% overall diagnostic accuracy . (see Table 2 and 3)
As a locator of PTB opacities and pulmonary cavity, the trained detector demonstrated 84.04% sensitivity, 98.04% specificity, and 95% overall diagnostic accuracy. (see Table 4 and 5)

## DISCUSSION

The trained detector performed better as a screening tool than a locator, achieving 92.11% sensitivity and 87.11% specificity. This is due to the fact that all radiographs with a true positive finding, whether there were also false positives and false negatives within the same radiograph, were counted as true positive. This parameter was made more lenient to maximize sensitivity, which is the goal of a screening tool.

In comparison, analysis of the detector as a locator showed slightly lower sensitivity of 84.04%, while specificity was higher at 98.04%. There were significantly more false negatives in this analysis. This meant that the detector failed to recognize certain opacity configurations (see Figure 6), thereby decreasing sensitivity. On the other hand, specificity was markedly increased to 98.04%. This can be attributed to increased representation of areas with negative findings, due to the shift to the unit of analysis to the one-sixth lung region. This amplified the true negative regions to a total of 501, increasing specificity.

There were few reasons for false positive findings (see Figure 7). Some false positives were due to the detector mistaking other lung opacities, such as pneumonia or pulmonary congestion, for PTB. Another common source of false positives was the stomach bubble being mistaken for a PTB opacity or cavity.

As a screening tool, the trained detector may only be compared to other studies that used algorithms for image classification (see Table 6). In comparison with studies utilizing histogram analysis, the trained detector was mostly at par in terms of sensitivity, exhibiting slightly lower sensitivity than that by Rohmah et al., which had a sensitivity of 93.3%, but exhibiting slightly higher sensitivity than that by Tan et al., which had a sensitivity of 91%.

In comparison with studies utilizing CNN, the detector was only slightly less accurate than that by Hwang et al., which achieved 90.3% accuracy as opposed to this study's accuracy of 89%. However it was markedly less sensitive and specific than that by Lakhani et al., which had a sensitivity and specificity of 97.3% and 100%, respectively. This may be attributed to a smaller number of training samples used in this study, as compared to these studies. The study by Hwang utilized 7500 images, while the study by Lakhani used 1016 images, as opposed to the 554 used in this study.

Compared with the above-mentioned studies which used histogram analysis or CNN, the trained detector had lower specificity and accuracy across all studies, regardless of algorithm (see Table 6). This may be attributed to the fact that, aside from Rohmah et al., other studies used only either normal chest radiographs or radiographs with PTB in their testing dataset. In contrast, this study incorporated radiographs with other pathologic findings such as pneumonia or congestion in the testing phase. This caused more false negatives, with the detector mistaking other opacities for PTB. However, this approach is more reflective of real-world situations.

Pande et al[2] cited 8 studies in total pertaining to CAD4TB. The detector in this study demonstrated greater sensitivity than 6 of 8 studies, and greater specificity than 7 of 8 studies (see Table 6).

The study by Xu et al., which utilized a combination of Gaussian-model-based template matching (GTM), local binary patterns (LBP), and histogram of oriented gradients (HOG), is the only other published research that also attempted location of PTB opacities. As a locator, the trained detector in this study had markedly higher sensitivity, specificity, and accuracy than that by Xu et al (see Table 7). This may be attributed to higher number of training samples. Xu et al. only used 30 training samples, as opposed this study which utilized 554 training samples. Another reason for better performance may be due to the Faster R-CNN algorithm being more robust in object detection than GTM, LBP, and HOG.

Some studies such as that by Hwang et al., Lakhani et al., and Pande et al., incorporated a microbiologic basis for PTB in their studies. A limitation and weakness of this study is the lack of any microbiologic basis.

## CONCLUSION AND RECOMMENDATIONS

This study has demonstrated the feasibility of training a detector for PTB and pulmonary cavities using the Faster R-CNN algorithm. Performance in terms of sensitivity, specificity and accuracy were comparable to and exceeded that of similar studies, and even that of commercially available software.

This study is the first of its kind to utilize Faster R-CNN in the detection of PTB opacities and pulmonary cavities. Faster R-CNN is a general object detection algorithm, and this study may be used as a template for the creation and assessment of detectors for other findings on medical images.

Performance of the detector may be improved by incorporating the following in future research:

- The number of training images may be increased to increase the variety of findings that the detector is exposed. This may decrease the number of false negative findings.
- The Faster R-CNN algorithm may be combined with a lung segmentation algorithm to prevent out-of-bounds findings. This may decrease the number of false positive findings.
- Using a microbiologic basis for establishing PTB along with chest radiographs would increase research validity.

## REFERENCES

1. 2016 National Tuberculosis Prevalence Survey Results [Internet]. 24th Annual PhilCAT Convention; Philippine Coalition Against Tuberculosis; 2017 Aug 17; Crowne Plaza, Robinsons Galleria, Ortigas Center, Quezon City, Philippines. Available from: http://www.philcat.org/PDFFiles/2.NTPSPhilCAT_17Aug2017_Dr.%20Lansang.pdf
2. Pande T, Cohen C, Pai M, Ahmad Khan F. Computer-aided detection of pulmonary tuberculosis on digital chest radiographs: a systematic review. Int J Tuberc Lung Dis. 2016;20(9):1226–30.
3. Von Zitzewitz G. Survey of neural networks in autonomous driving. 2017 Jul 9 [cited 2019 Jun 22]; Available from: http://dx.doi.org/
4. Hwang S, Kim H-E, Jeong J, Kim H-J. A novel approach for tuberculosis screening based on deep convolutional neural networks. In: Medical Imaging 2016: Computer-Aided Diagnosis [Internet]. 2016. Available from: http://dx.doi.org/10.1117/12.2216198
5. Lakhani P, Sundaram B. Deep Learning at Chest Radiography: Automated Classification of Pulmonary Tuberculosis by Using Convolutional Neural Networks. Radiology. 2017 Aug;284(2):574–82.
6. Ren S, He K, Girshick R, Sun J. Faster R-CNN: Towards Real-Time Object Detection with Region Proposal Networks [Internet]. 2015 [cited 2019 Mar 6]. Available from: http://arxiv.org/abs/1506.01497
7. MicroDicom - Free DICOM viewer and software [Internet]. [cited 2019 Mar 7]. Available from: http://www.microdicom.com/
8. GIMP [Internet]. GIMP. [cited 2019 Mar 7]. Available from: https://www.gimp.org/

9. tzutalin. tzutalin/labelImg [Internet]. GitHub. [cited 2019 Mar 7]. Available from: https://github.com/tzutalin/labelImg

10. Evan Juras. How to train a TensorFlow Object Detection Classifier for multiple object detection on Windows [Internet]. Github; 2018 [cited 2019 Mar 9]. Available from: https://github.com/EdjeElectronics/TensorFlow-Object-Detection-API-Tutorial-Train-Multiple-Objects-Windows-10

11. Mohamad Adam Bujang THA. Requirements for Minimum Sample Size for Sensitivity and Specificity Analysis. J Clin Diagn Res. 2016 Oct;10(10):YE01.

12. OpenCV library [Internet]. [cited 2019 Mar 10]. Available from: https://opencv.org/

13. Rohmah RN, Susanto A, Soesanti I. Lung tuberculosis identification based on statistical feature of thoracic X-ray [Internet]. 2013 International Conference on QiR. 2013. Available from: http://dx.doi.org/10.1109/qir.2013.6632528

14. Tan JH, Acharya UR, Tan C, Abraham KT, Lim CM. Computer-assisted diagnosis of tuberculosis: a first order statistical approach to chest radiograph. J Med Syst. 2012 Oct;36(5):2751–9.

15. Maduskar P, Muyoyeta M, Ayles H, Hogeweg L, Peters-Bax L, van Ginneken B. Detection of tuberculosis using digital chest radiography: automated reading vs. interpretation by clinical officers. Int J Tuberc Lung Dis. 2013 Dec;17(12):1613–20.

16. Breuninger M, van Ginneken B, Philipsen RHHM, Mhimbira F, Hella JJ, Lwilla F, et al. Diagnostic accuracy of computer-aided detection of pulmonary tuberculosis in chest radiographs: a validation study from sub-Saharan Africa. PLoS One. 2014 Sep 5;9(9):e106381.

17. Xu T, Cheng I, Long R, Mandal M. Novel coarse-to-fine dual scale technique for tuberculosis cavity detection in chest radiographs [Internet]. Vol. 2013, EURASIP Journal on Image and Video Processing. 2013. Available from: http://dx.doi.org/10.1186/1687-5281-2013-3

## APPENDICES, TABLES AND FIGURES

### *Appendices*

**Appendix 1. Table for minimum sample size for sensitivity and specificity analysis**[11]

Part of the table for minimum sample size for sensitivity and specificity analysis by Bujang[11] is displayed below. The parameters used in this study are boxed in orange.

| n (Sensitivity) | | | | | | |
|---|---|---|---|---|---|---|
| Prev | $H_0$ | $H_a$ | Power | p-value | N1 | N |
| 30% | 0.50 | 0.60 | 0.804 | 0.047 | 199 | 663 |
| 30% | 0.50 | 0.70 | 0.810 | 0.044 | 49 | 163 |
| 30% | 0.50 | 0.80 | 0.804 | 0.041 | 20 | 67 |
| 30% | 0.50 | 0.90 | 0.889 | 0.039 | 12 | 40 |
| 30% | 0.60 | 0.70 | 0.801 | 0.048 | 181 | 603 |
| 30% | 0.60 | 0.80 | 0.826 | 0.034 | 45 | 150 |
| 30% | 0.60 | 0.90 | 0.885 | 0.035 | 19 | 63 |

| n (Specificity) | | | | | | |
|---|---|---|---|---|---|---|
| Perv | $H_0$ | $H_a$ | Power | p-value | N1 | N |
| 30% | 0.50 | 0.60 | 0.804 | 0.047 | 85 | 284 |
| 30% | 0.50 | 0.70 | 0.810 | 0.044 | 21 | 70 |
| 30% | 0.50 | 0.80 | 0.804 | 0.041 | 9 | 29 |
| 30% | 0.50 | 0.90 | 0.889 | 0.039 | 5 | 17 |
| 30% | 0.60 | 0.70 | 0.801 | 0.048 | 78 | 259 |
| 30% | 0.60 | 0.80 | 0.826 | 0.034 | 19 | 64 |
| 30% | 0.60 | 0.90 | 0.885 | 0.035 | 8 | 27 |

## Appendix 2. Sample of verification log sheet.

**Verification Logsheet**
**Computer-aided detection of PTB and pulmonary cavities on adult chest radiographs**

| Filename | Finding | Top y | Top x | Bottom y | Bottom x | % | Verification by Radiologist | Missed TB or cavity? Please specify location | Classification - to be filled up by investigator (TP, FP, TN, FP) |
|---|---|---|---|---|---|---|---|---|---|
| test001 | No cavity or PTB | | | | | | ✓ | | TN |
| test002 | No cavity or PTB | | | | | | ✓ | | TN |
| test003 | No cavity or PTB | | | | | | ✓ | | TN |
| test004 | No cavity or PTB | | | | | | ✓ | | TN |
| test005 | PTB | 216 | 312 | 296 | 384 | 100.00% | ✓ | | TP |
| | PTB | 106 | 128 | 198 | 210 | 100.00% | ✓ | | TP |
| | PTB | 213 | 307 | 325 | 396 | 99.89% | ✓ | | TP |
| | PTB | 109 | 70 | 286 | 221 | 96.53% | ✓ | | TP |
| | PTB | 185 | 337 | 244 | 387 | 88.47% | ✓ | | TP |
| test006 | No cavity or PTB | | | | | | ✓ | | TN |
| test007 | No cavity or PTB | | | | | | ✓ | | TN |
| test008 | No cavity or PTB | | | | | | ✓ | | TN |
| test009 | No cavity or PTB | | | | | | ✓ | | TN |
| test010 | PTB | 108 | 76 | 195 | 158 | 99.98% | ✓ | | TP |
| | PTB | 260 | 102 | 322 | 161 | 99.98% | ✓ | | TP |

***Figures***

**Figure 1. Flow diagram for training the Faster R-CNN detector**

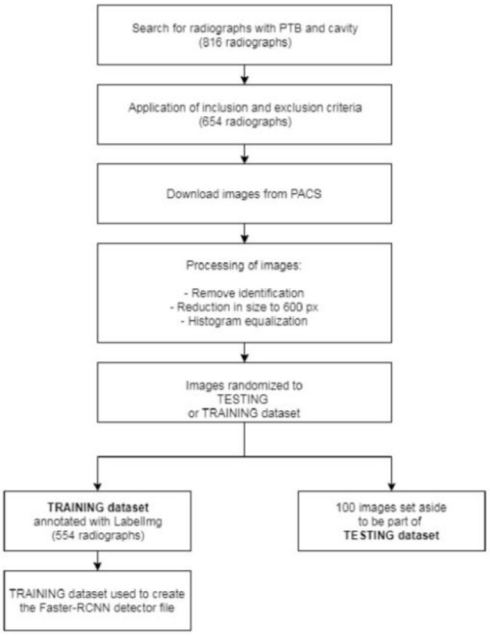


**Figure 2. Flow diagram for testing the Faster R-CNN detector**

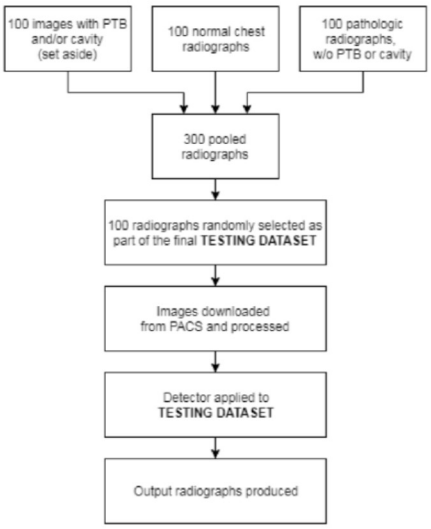

**Figure 3. Sample output radiographs demonstrating detection of PTB opacities and cavities.**
Each of the output radiographs below show correct detection of PTB opacities (boxed in green) and pulmonary cavities (boxed in yellow).

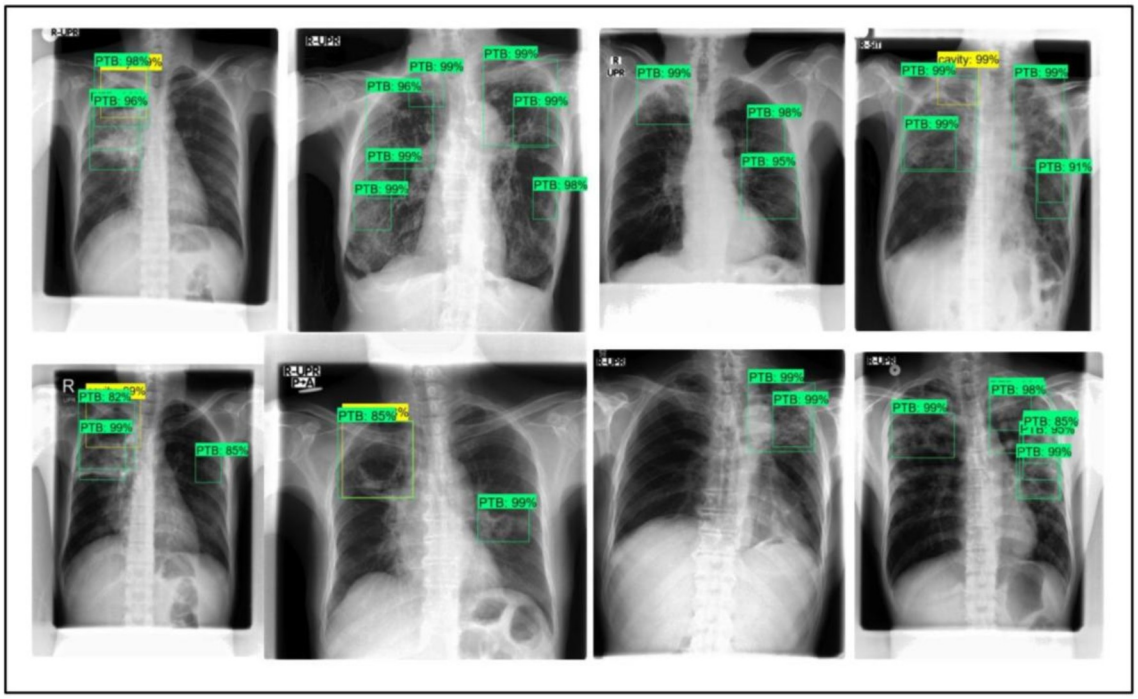

**Figure 4. Example radiographs for classifications for analysis as a screening tool.**
*(In order of images from the left)*
*1st image:* True Negative radiograph shows no identified PTB opacities or cavity.
*2nd image:* True Positive radiograph shows PTB opacities correctly identified by the detector.
*3rd image:* False Negative radiograph shows missed PTB opacities (encircled in red) in the right upper lung, which was not identified by the detector.
*4th image:* False Positive radiograph shows the stomach bubble misidentified as PTB opacity.

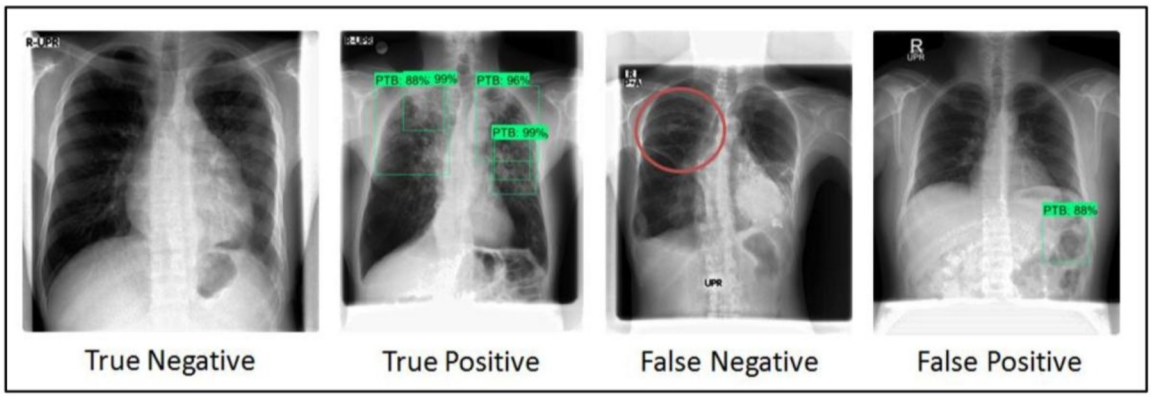

**Figure 5. Sample radiograph for classification for analysis as a locator.**

The radiograph on the left shows PTB opacities, as identified by the detector. The radiograph on the right shows the same radiograph with blue translucent overlay dividing each lung into upper, middle, and lower regions. Each lung region is classified according to the bounding boxes within it. In this example, bounding boxes are seen occupying the both upper to mid lungs, and are hence classified as true positives. Lower lungs have no bounding boxes, and are classified as true negatives.

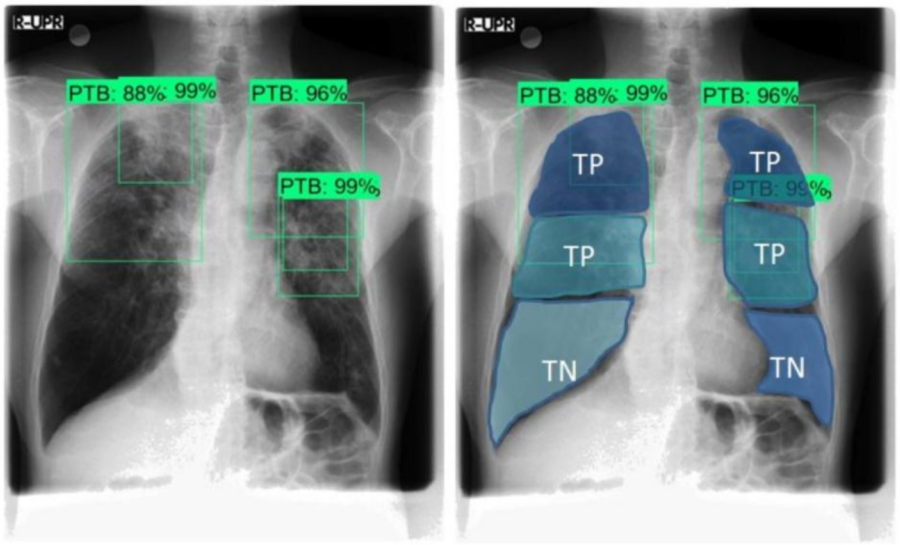


**Figure 6. Sample radiographs exhibiting false negatives.**

The radiograph on the left exhibits PTB opacities in the right upper lung. The radiograph on the right shows subtle PTB opacities in both upper lungs. The trained detector did not place any bounding boxes around these findings, and were thus considered missed by the detector.

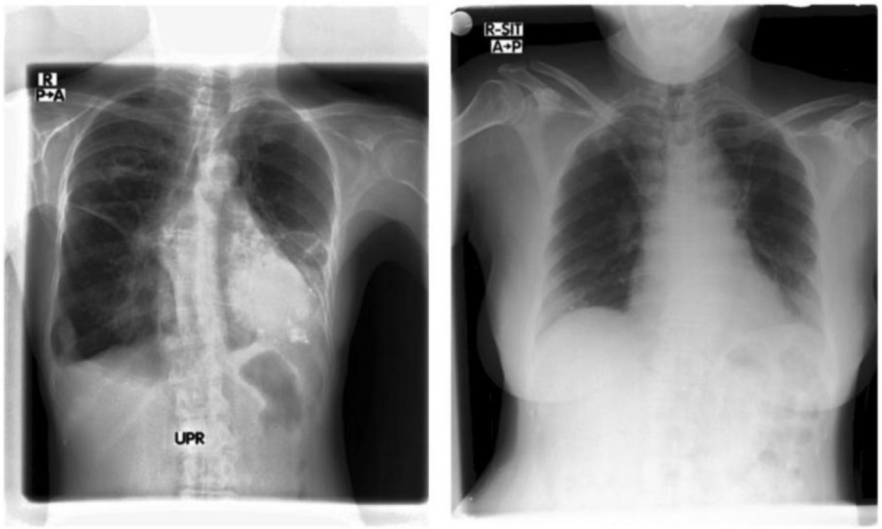

**Figure 7. Sample radiographs exhibiting false positives.**

*Left radiograph:* Radiograph exhibits pneumonia mistaken for PTB by the detector.
*Middle and right radiographs:* Radiographs show the stomach bubble as mistaken for PTB and cavity, respectively.

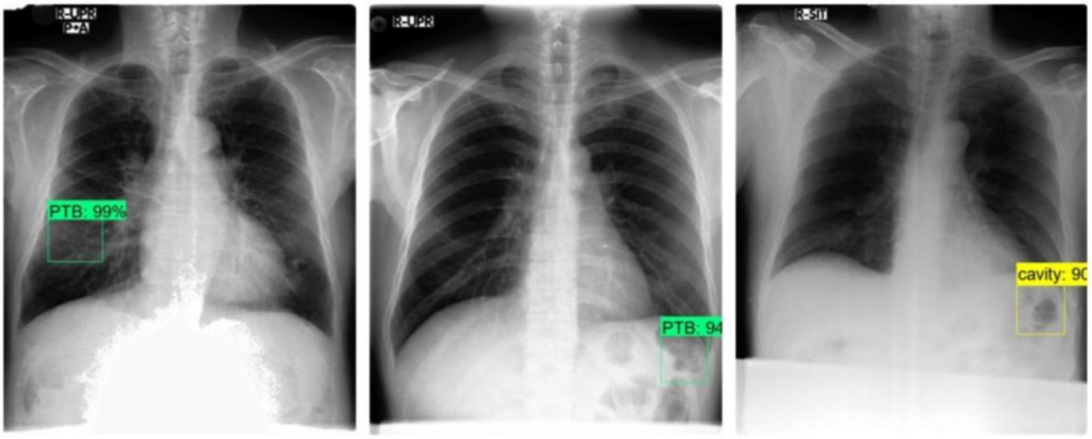


## Tables

**Table 1. Composition of final testing dataset.**

| Classification | Number of radiographs |
|---|---|
| **Negative chest radiographs** | **36** |
| **Radiographs with PTB opacities and/or cavity** | **32** |
| Radiographs with PTB opacities without cavity | 4 |
| Radiographs with PTB opacities and cavity | 28 |
| **Pathologic Radiographs without PTB and cavity** | **32** |
| Pneumonia | 21 |
| Pleural effusion | 5 |
| Pulmonary congestion | 2 |
| Bronchitis/bronchiectasis | 1 |
| Pulmonary nodule | 1 |
| Fibrosis | 1 |
| Subsegmental atelectasis | 1 |
| **GRAND TOTAL** | **100** |

**Table 2. 2 x 2 Contingency table for analysis as a screening tool.**

| | | Radiographs verified by panel of radiologists | | |
|---|---|---|---|---|
| | | **Positive** | **Negative** | **TOTAL** |
| Radiographs identified by the detector | **Positive** | 35 | 8 | 43 |
| | **Negative** | 3 | 54 | 57 |
| | **TOTAL** | 38 | 62 | 100 |

**Table 3. Summary table for analysis as a screening tool.**

| Parameter | Value | Lower-Upper 95% Confidence Intervals |
|---|---|---|
| Sensitivity | 92.11% | 79.2, 97.28% |
| Specificity | 87.10% | 76.55, 93.31% |
| Accuracy | 89.00% | 81.37, 93.75% |

**Table 4. 2 x 2 Contingency table for analysis as a locator of PTB opacities and cavity**

| | | Lung regions verified by panel of radiologists | | |
|---|---|---|---|---|
| | | **Positive** | **Negative** | **TOTAL** |
| Lung regions identified by the detector | **Positive** | 79 | 10 | 89 |
| | **Negative** | 15 | 501 | 516 |
| | **TOTAL** | 94 | 511 | 605 |

**Table 5. Summary table for analysis as a locator of PTB opacities and cavity**

| Parameter | Value | Lower-Upper 95% Confidence Intervals |
|---|---|---|
| Sensitivity | 84.04% | 75.33, 90.08% |
| Specificity | 98.04% | 96.44, 98.93% |
| Accuracy | 95.87% | 93.97, 97.19% |

**Table 6. Summary table of studies on computer-aided detection of PTB, as a screening tool.**

| Author, Year | Algorithm used | Training samples | Sensitivity | Specificity | Accuracy |
|---|---|---|---|---|---|
| This study, as a screening tool | Faster R-CNN⁺ | 554 | 92.11% | 87.1% | 89.00 % |
| Rohmah et al. 2013.[13] | Histogram analysis | 50 | 93.3 % | 97.5 % | 95.70 % |
| Tan et al. 2012.[14] | Histogram analysis | 64 | 91% | 95.4% | 92.9% |
| Hwang et al. 2016.[4] | CNN‡ | 7500 | | | 90.3% |
| Lakhani et al. 2017.[5] | CNN‡ | 1016 | 97.3% | 100% | |
| Pande et al. 2016.[2] | Proprietary | Undisclosed | 1: 86% | 1: 41% | |
| Includes the following studies:<br>1: Maduskar, et al.[15]<br>2: Muyoyeta et al.[15]<br>3-8: Breuninger, et al.[16] | | | 2: 100%<br>3: 95%<br>4: 91%<br>5: 85%<br>6: 77%<br>7: 62%<br>8: 47% | 2: 23%<br>3: 33%<br>4: 52%<br>5: 69%<br>6: 79%<br>7: 85%<br>8: 94% | |

⁺ R-CNN = Region Convolutional Neural Network, ‡CNN = Convolutional Neural Network

**Table 7. Summary table of studies on computer-aided detection of PTB, as a locator.**

| Author, Year | Algorithm used | Training samples | Sensitivity | Specificity | Accuracy |
|---|---|---|---|---|---|
| This study, as a locator | Faster R-CNN⁺ | 554 | 84.04% | 98.04% | 95.87 % |
| Xu et al. 2013.[17] | GTM, LBP, HOG‡ | 30 | 69.4 - 78.8% | 81.6 - 86.8% | 75.5 - 82.8% |

⁺ R-CNN = Region Convolutional Neural Network
‡GTM = Gaussian-model-based template matching, LBP = local binary patterns, HOG = histogram of oriented gradients